Composites Science and Technology 218 (2022) 109201

Contents lists available at ScienceDirect

Composites Science and Technology

journal homepage: www.elsevier.com/locate/compscitech

Enhanced thermal and electrical properties by Ag nanoparticles decorated GO-CNT nanostructures in PEEK composites

Chenxi Hu [a,b], Tianhui Liu [a], Nigel Neate [a,c], Michael Fay [a,c], Xianghui Hou [a], David Grant [a], Fang Xu [a,*]

[a] Advanced Materials Research Group, Faculty of Engineering, University of Nottingham, NG7 2RD, UK
[b] College of Science, Civil Aviation University of China, Tianjin, 300300, China
[c] Nanoscale and Microscale Research Centre (nmRC), University of Nottingham, University Park, Nottingham, NG7 2RD, UK

ARTICLE INFO

Keywords:
Carbon nanotubes
Graphene and other 2D-materials
Polymer-matrix composites (PMCs)
Electrical properties
Thermal properties

ABSTRACT

A nanostructure of graphene oxide (GO) and carbon nanotubes (CNTs) decorated with silver nanoparticles (AgGNT) has been prepared via a molecular-level-mixing (MLM) method followed by a subsequent freeze-drying and reduction process. The obtained well-dispersed AgGNT nanostructures were then applied as fillers to reinforce the poly(ether ether ketone) (PEEK) matrix. AgGNT-PEEK composites have then demonstrated excellent electrical and thermal conduction performances as well as high thermal durability compared with pure PEEK and its pure Ag or GO-CNT (GNT) enhanced composites. Owing to the unique morphology of AgGNT nanostructures, which made them uniformly dispersed in the PEEK matrix and formed a 3D network structure, the AgGNT-PEEK composites displayed 60% higher thermal conductivity and around 10^9 times better electrical conduction performance than pure PEEK, and superior thermal durability even above the melting temperature of pure PEEK. Thus, the AgGNT-PEEK composites have shown great potential for applications such as semiconductors, high-temperature electrical applications, aerospace, and automobile materials.

1. Introduction

Poly(ether ether ketone) (PEEK) and its relevant composites have become increasingly popular since their commercialisations in 1981 [1]. As a semi-crystalline thermoplastic polymer, PEEK shows great potential in various applications due to its excellent thermal and chemical stability, as well as outstanding mechanical properties and moisture resistance [2]. Thus, PEEK and its composites have been explored to serve in various fields, such as aerospace, machinery, automobile, and electronic industries. However, PEEK cannot be applied as a long time strength material when exposed to an environment hotter than the heat-deflection temperature of PEEK (around 156 °C) [3], although it shows the glass-transition temperature at 143 °C and high melting temperature (generally above 300 °C) [2,4–7]. Meanwhile, like all other polymer materials, PEEK has been regarded as an insulator, which would hinder the heat and electrostatic charge flows and restrict its further application. To make the PEEK more widely used, different strategies have been explored to improve the thermal and/or electrical conductivity as well as the thermal durability based on PEEK's inherent properties. Amongst them, the introduction of different fillers to prepare polymer matrix composites (PMC) has become a promising way to tailor the properties of composites.

Carbon materials, such as the one-dimensional carbon nanotubes (CNTs) and two-dimensional graphene, have attracted increasing attention in preparing advanced materials due to their unique structures and properties, like high electrical conductivity and impressive thermal conductivity [7–10]. Thus, the addition of carbon materials as fillers in PEEK has become a promising approach to enhance PEEK-based materials and has already been reported in previous research. The use of CVD-grown multi-walls CNTs as reinforcements in PEEK was reported by Hoa et al. [11], which displayed increased electrical conductivity from around 10^{-13} to 10^{-3} S m^{-1}. The graphene reinforced PEEK nanocomposites reported by Tewatia also demonstrated improved storage modulus [12]. The GO and CNT combined nanostructure was also investigated as fillers and showed improved thermal conductivity of PEEK from 0.18 to 0.35 W $m^{-1}K^{-1}$ [2]. However, apparent agglomeration of carbon materials, which resulted from the strong π-π interactions that appeared between each carbon layer, still could be

* Corresponding author.
E-mail address: Fang.Xu@nottingham.ac.uk (F. Xu).

https://doi.org/10.1016/j.compscitech.2021.109201
Received 24 August 2021; Received in revised form 29 November 2021; Accepted 4 December 2021
Available online 7 December 2021

observed in the PEEK matrix and hence reduced the final properties.

Meanwhile, the addition of metallic fillers (i.e. Ag, Cu, and Co) is also regarded as an efficient approach to enhance PMCs' properties. Cu and Ag nanowires fillers were investigated in Tetradecanol by Zeng et al. and the thermal conductivity of the products increased with the increase of loading [13,14]. Rivière and co-workers have studied different kinds of Ag nanostructures as fillers (such as nanowires and nanospheres) and their influences on the electrical and thermal conductivity of PEEK with different filler content [15,16]. The results showed that the Ag nanowires composite displayed a lower electrical percolation threshold of around 0.55 vol% compared with the Ag spherical particles composite whose value is 10.80 vol%. It is believed that the pathways could be much more easily formed with Ag nanowires in the PEEK matrix when compared with Ag spherical particles. However, the uniform dispersion of metallic fillers in the matrix has become a challenge. The high-performance composites in these researches always come with a high ratio of metallic fillers as well as high costs. Therefore, advanced strategies are needed to further improve the unsatisfied performance of such PEEK-based composites. To generate uniform structures of fillers in the matrix should be a promising strategy to further reinforce the performance of the matrix. To the best of our knowledge, little research has been done in combining the metallic fillers in PEEK matrix composites, in particular, there is no systematic investigation of metal-carbon nanostructure with 3D distribution to reinforce the PEEK matrix composites.

In this study, the Ag nanoparticles decorated GO-CNT (GNT) nanostructures (AgGNT) have been prepared through a novel molecular-level-mixing (MLM) method with the subsequent freeze-drying and reduction processes. The well-dispersed graphene-layer-like GNT nanostructure with a uniform decoration of Ag nanoparticles could prevent the agglomeration of Ag and keep a well-dispersed morphology during the subsequent composite preparation process. The as-prepared samples then acted as the reinforcements in the PEEK matrix. The structure and morphology characterisation, and the properties evaluation (including thermal and electrical properties) of the obtained composites were then performed and the relevant results were discussed.

2. Experimental

2.1. Materials

Graphene oxide (GO) dispersions were purchased from William Blythe Limited Limited, UK, carbon nanotubes (CNTs) were purchased from Carbon Nanotubes Plus, US, silver acetate (CH_3COOAg), sulfuric acid (H_2SO_4) and acetone were purchased from Sigma-Aldrich, while nitric acid (HNO_3) was purchased from Fisher Scientific. PEEK was provided by Vicote coatings. Liquid nitrogen and Ar/H_2 mixed gas (5% H_2 + 95% Ar) were supplied by BOC Gas Cylinders.

2.2. Acid treatment of CNTs

The purchased CNTs were firstly acid-treated. Specifically, 0.5 g CNTs were weighed and placed in a flask, 10 mL HNO_3, and 5 mL H_2SO_4 were then slowly poured into it. After heating in an oil bath with magnetic stirring, the flask was kept at 130 °C with a reflux system for 25 min. The acid-treated CNTs were then filtrated, rinsed with distilled water, and dried in a vacuum oven overnight.

2.3. Preparation of Ag decorated GNT (AgGNT) nanostructures

The Ag decorated GNT nanostructures were obtained through the MLM method with the subsequent freeze-drying and reduction process (as shown in Fig. 1). A certain amount of CH_3COOAg was dissolved in 50 mL H_2O with magnetic stirring, while CNTs and GOs with a ratio of 1:1 were mixed and dispersed under ultra-sonication for half an hour in a beaker. The obtained carbon mixture was then poured into the prepared silver solution with a weight ratio of Ag to C (including carbon nanotubes and graphene) as 8: 2 and stirred for another 2 h. After completely mixing, the suspension was quickly transferred into a liquid nitrogen (LN_2) atmosphere for fast freezing. The precursor was then obtained through the freeze-drying approach (Labconco FreeZone 76705 freeze dry system) at −55 °C and 0.024 mBar. The freeze-dried precursors were subsequently reduced under the H_2/Ar atmosphere at 200 °C in a tube furnace for 3 h. The pure GNT sample was prepared in

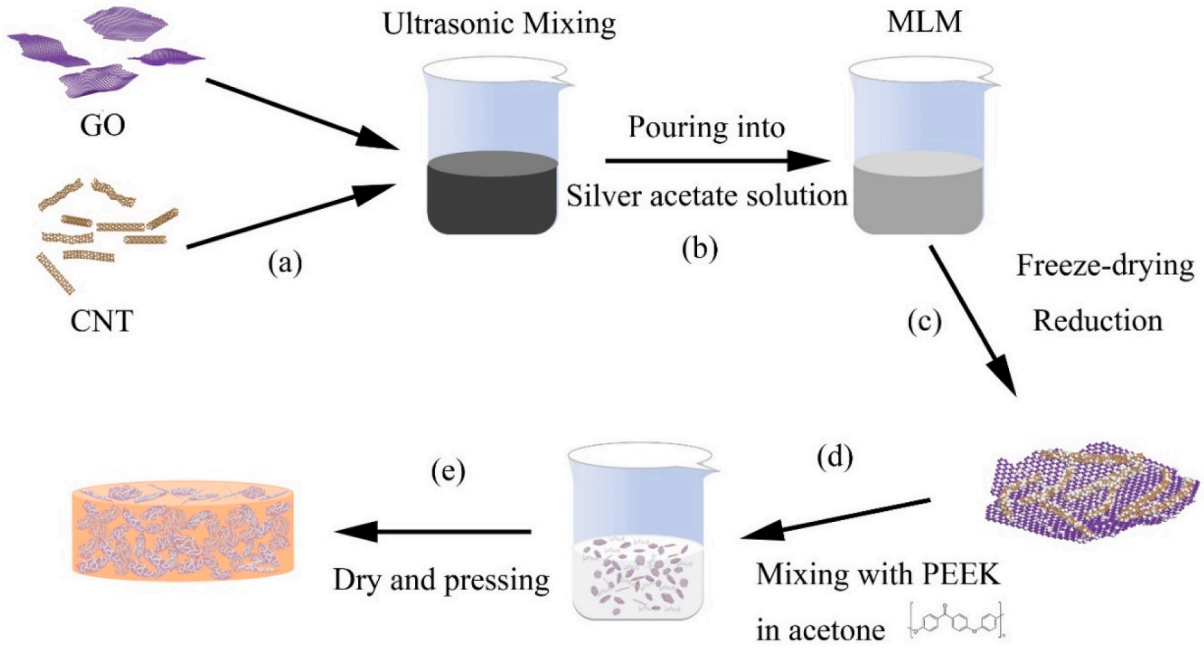

Fig. 1. Schematic diagram of the preparation of AgGNT-PEEK composites through (a) ultrasonication mixing of GO and CNTs, (b) MLM with GNT and silver salt solutions, (c) subsequent freeze-drying and reduction process to prepare AgGNT nanostructures, (d) mixing of AgGNT and PEEK powders, and (e) pressing of mixed powders into a disc.

the same way as the AgGNT sample without the addition of CH_3COOAg, while the pure Ag sample was obtained in the same way as the AgGNT sample just without the addition of GNT.

2.4. Composites fabrication

To prepare the PEEK-based composites, the as-prepared AgGNT nanostructures were mixed with PEEK powders, and the schematic diagram (Fig. 1) displays this process. Firstly, the AgGNT nanostructures and PEEK powders were ultrasonically dispersed in acetone separately, and then poured together with a weight ratio of 30:70 (AgGNT: PEEK) under magnetically stirring for 1 h. The calculated volume ratio of Ag and C from the nanostructures (including carbon nanotubes and graphene) in the composites are 3.9 vol% for Ag and 5 vol% for C from the nanostructures. Secondly, the well-dispersed solution was then stirred and heated at 90 °C to remove the acetone. Thirdly, the obtained powders were transferred into an oven and completely dried at 120 °C overnight. Finally, the mixed powders were pre-pressed into 13 mm diameter disc with a die, and the discs were heated at 370 °C for 2 h in an oven. The obtained discs were named as AgGNT-PEEK composites and collected for further investigation. Meanwhile, pure GNT and pure Ag samples were also separately mixed with PEEK as reference samples with the same weight amount of fillers as AgGNT. As the weight ratio of Ag: C in AgGNT nanostructures is 8: 2 and the weight percentage of AgGNT fillers in final composites is 30 wt%, the prepared ratio of GNT in as-prepared composites (named as GNT-PEEK) is 6 wt % and that of Ag particles in as-prepared composites (Ag-PEEK) is 24 wt%. In addition, the obtained discs were prepared through the same process as the AgGNT-PEEK composite.

2.5. Characterisation

The X-ray diffraction (XRD) scanning results were obtained through the Bruker D8 Advance system (operated at 40 kV and 35 mA) using Cu K-α radiation as the X-Ray source, between 5 and 80° 2θ range at a scanning step of 0.01°, and the time per step is 0.12s. The morphologies of prepared powders (including pure GNT, pure Ag, and AgGNT samples) were obtained by JEOL 7100 field emission gun scanning electron microscope (SEM) with the working voltage of 15 kV, while the PEEK based composites were observed through the cryogenic fracture surfaces, which were obtained by LN_2 freezing and smashed by a hammer and then coated with 10 nm carbon using a sputtering device. A JEOL 2100+ Transmission Electron Microscopy (TEM), equipped with a Gatan Ultrascan 1000XP detector and Gatan Microscopy Suite software operating at a working voltage of 200 kV was used to obtain TEM and HRTEM images of AgGNT nanostructures, while the images of PEEK based composites were obtained under 80 kV. The TEM sample of AgGNT nanostuctures was prepared by dispersing the as-prepared powders in ethanol under sonication and then dropping onto holey carbon TEM grids, while all composite samples were cut using a microtome with a fine diamond blade into thin films of ca. 100 nm for observing. X-ray photoelectron spectroscopy (XPS) was carried out on a VG ESCALab Mark II spectrometer machine using Al K-α X-ray as an excitation source with a wavelength of 1486.6 eV. It was performed with an anode voltage of 12 kV and an emission current of 20 mA.

Thermogravimetric (TGA) measurements were carried out using TA Q600 SDT. The AgGNT sample powders were tested from 50 to 900 °C in air, while the PEEK-based composites were measured from 50 to 900 °C under Ar both with a ramp rate of 10 °C min^{-1}. Differential scanning calorimetry (DSC) was introduced to analyse the melting behaviours with TA DSC2500. The measurements were carried out under the N_2 atmosphere, and the samples which had the average mass of around 10 mg were heated up from 30 to 380 °C at a ramping rate of 10 °C min^{-1} in the sealed aluminium pans.

The thermal diffusivities (α) of all the PEEK-based composites were measured by NETZSCH Light Flash Apparatus (LFA) 467 Hyper Flash instrument at room temperature. Density (ρ) of the as-prepared discs were obtained through the Archimedes' principle. The specific heat capacity (C_p) of all PEEK based disc was recorded by TA DSC2500. The thermal conductivities of these samples were then calculated by the equation: $K = \alpha \times \rho \times C_p$.

The electrochemical impedance spectroscopy (EIS) tests were measured by ModuLab XM Materials Test System (Solartron, Hampshire, U.K.). The EIS curves were measured at room temperature over the frequency range of 0.01–1 MHz. Impedance plots were analysed using the Zview software (Scribner Associates, Inc). The values of electrical resistivity can be obtained from the intercept of the corresponding semicircle on the real part of the impedance.

The thermal-mechanical analysis (TMA) was adopted to analyse the thermal durability of the PEEK composites with TMA Q400 from room temperature to 400 °C with 10 °C min^{-1} under the N_2 atmosphere, and the applied pressure on the disc was increased from 10^3 to 10^4 Pa.

3. Results and discussion

3.1. Structure and morphology characterisation

The XRD patterns of AgGNT, pure Ag, and pure GNT samples are displayed in Fig. 2a. Three strong diffraction peaks at 2θ of 38.1°, 44.3°, and 64.2° can be observed in the XRD patterns of AgGNT and pure Ag samples, indicating the (111), (200) and (220) planes of Ag (ICDD PDF No. 00-04-0783). No obvious sharp diffraction peak can be observed in pure GNT samples (Peak 3) except for a broad peak that can be attributed to the existence of carbon material ranging from 25 to 45° [17]. For pure Ag and AgGNT composites (curve 1 and 2), the XRD patterns of AgGNT composites also show a minor broad peak around 30° (insert picture of Fig. 2a) compared with pure Ag sample, which further confirms the existence of both Ag and GNT contents in AgGNT samples. No other peaks in the patterns of AgGNT and pure Ag samples confirms that both the precursors of AgGNT and Ag were completely reduced to metal Ag under the Ar/H_2 atmosphere at 200 °C for 3 h. The thermogravimetric (TGA) result of AgGNT nanostructures from 50 to 900 °C in air is shown in Fig. S1, the weight decrease starting from around 200 °C can be ascribed to the burning of carbon content, which corresponds to the exothermic peak in the DSC curve as well. The remaining weight percentage is 82.5 wt%. The calculated Ag:C weight ratio is close to 8:2, which is consistent with the initial weight ratio in the sample preparation procedure.

The XPS spectra of AgGNT and pure GNT samples are illustrated in Fig. 2b–d. In Fig. 2b, the survey scan spectra of both samples display the characteristic peak of C1s and O1s, which confirm the existence of C and O elements in both samples. In addition, Ag3d and Ag3p characteristic peaks can be observed in the survey scan of AgGNT sample, which demonstrates the Ag element in the AgGNT nanostructures. The C1s spectra and their deconvolution peaks of pure GNT and AgGNT are displayed in Fig. 2 c and d, respectively. For the deconvolution peaks of pure GNT samples (Fig. 2c), the C1s characteristic peak can be deconvoluted into five peaks, the sp^2 hybridized C located at 284.6 eV, the defect-containing sp^2 hybridized C at 285 eV, the *C*–O (ether bonds) at 286.3 eV, the C═O groups (ketone bonds) at 288.9 eV and the sp^2 hybrid orbit of benzene plane at 291.5 eV [18]. The existence of such oxygen contained peaks demonstrates the functional groups (such as carboxyl and hydroxyl groups) successfully attached on the surface of CNTs and GOs. These functional groups are believed not only to prevent the agglomeration between CNTs and GOs due to the electrostatic repulsion by the negative charge of each other [19] but also to provide abundant sites for metal ions nucleation. It is interesting to find that the C1s deconvolution peaks of AgGNT nanostructures show similar peaks as pure GNT samples. The appearance of the defect-containing sp2 hybridized C should come from the sp2 hybridized C as a result of the reduction process in the preparation procedures [20,21].

To investigate the morphology of the AgGNT, pure Ag and pure GNT

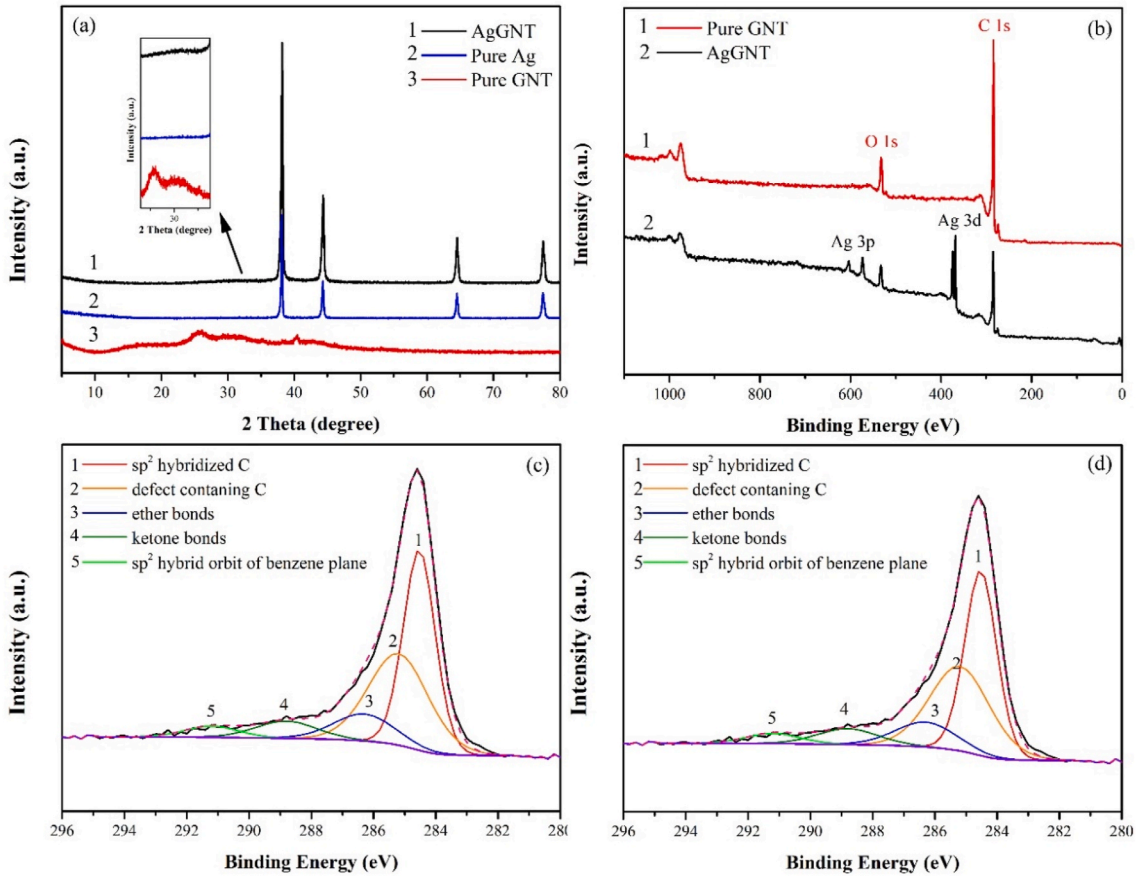

Fig. 2. (a) XRD patterns of AgGNT nanostructures, pure Ag and pure GNT, (b) XPS survey scan of pure GNT and AgGNT sample, C 1s spectra of pure GNT (c) and AgGNT (d).

samples, SEM and TEM images are shown in Fig. 3 and Fig. S2. Fig. 3a displays the AgGNT nanostructures with well-dispersed graphene-layer-like structures. No obvious agglomeration could be observed, which can be attributed to the freeze-drying process that largely kept the well-dispersed structure [22]. In the higher resolution image, the uniform distribution of Ag nanoparticles can be found on the graphene layer (Fig. 3b) and the surface of CNT walls (Fig. 3c). The particle size of the Ag nanoparticles coated on GNTs mainly ranges from 10 to 50 nm, while there are also few large particles ca. 100 nm. In the TEM image of AgGNT nanostructures (Fig. 3d), the Ag nanoparticles can be easily detected as high contrast (dark) features, while the graphene and CNTs are low contrast (light). In the insert image of Fig. 3d, four obvious ring patterns from the selected area electron diffraction (SAED) can be ascribed to the (111), (200), (220) and (311) planes of Ag, which is also consistent with the XRD results (Fig. 2a). In the HRTEM (Fig. 3e), an Ag nanoparticle can be observed attaching onto the surface of an MWCNT. The typical lattice fringe spacing is measured to be 0.24 nm, which can be ascribed to the (111) crystal plane of Ag. As the reference samples, the SEM images of pure Ag and GNT samples are illustrated in Fig. S2. The pure Ag particles can be found agglomerated even after a similar freeze-drying process (Figs. S2a and b), while the obtained Ag particles also show the particle size of over 100 nm, significantly larger than the particles decorating GNT hybrids. Meanwhile, the morphology of pure GNT sample shows a similar structure to AgGNT nanostructures. The graphene-layer-like structure can be observed (Fig. S2c). In the high-resolution image (Fig. S2d), CNTs are found attached on the surface of the graphene layer, which can be attributed to the $\pi-\pi$ interaction as well as the hydrogen and chemical bonds between CNT walls and graphene layers. Thus, it can be concluded that the graphene-layer-like structure of GNT sample was successfully obtained through the freeze-drying method, and the Ag nanoparticles were uniformly decorated on the surface of GNT structures. The introduction of GNT also effectively prevented the agglomeration of Ag particles.

After the preparation of PEEK-based composites, the XRD patterns of pure PEEK, GNT-PEEK composite, Ag-PEEK composite, and AgGNT-PEEK composite are displayed in Fig. 4. For the XRD pattern of pure PEEK (Fig. 4a), four obvious diffraction peaks located at 18.8°, 20.8°, 22.8° and 28.9° match well with the diffraction peaks of PEEK, which are corresponded to the (110), (111), (200), and (211) planes of PEEK. The GNT-PEEK composite (Fig. 4b) displays a similar XRD pattern as pure PEEK as the pure GNT didn't show an intense diffraction peak (Fig. 2c). The XRD patterns of Ag-PEEK and AgGNT-PEEK composites show prominent diffraction peaks of the Ag phase, indicating the existence of the Ag phase in both composites. Meanwhile, the characteristic peaks of PEEK also can be observed in both samples but not intensive.

The SEM images of cross-sections of obtained composites are shown in Fig. 5 and Fig. S3. A typical secondary electron (SE) image of pure PEEK is displayed in Fig. 5a. A squamous-like morphology can be observed on the cross-section [23], while a similar morphology is recorded in the backscattering (BSE) image (Fig. 5b). For the AgGNT-PEEK composites, the SE image (Fig. 5c) shows a rougher fracture surface compared with pure PEEK composites (Fig. 5a). In the BSE image (Fig. 5d), a much clearer contrast can be detected among the fracture surface as the silver nanoparticles could show brighter contrast due to the higher molar weight. Taking the morphology of AgGNT nanostructures (Fig. 3 a and b) into account, it can be considered that the AgGNT nanostructures are uniformly distributed among the PEEK matrix. The AgGNT nanostructures can be regarded to form a 3-dimensional (3D) network in the PEEK matrix. As the reference sample, the SE and BSE images of PEEK-GNT composites are illustrated in Fig. S3 a

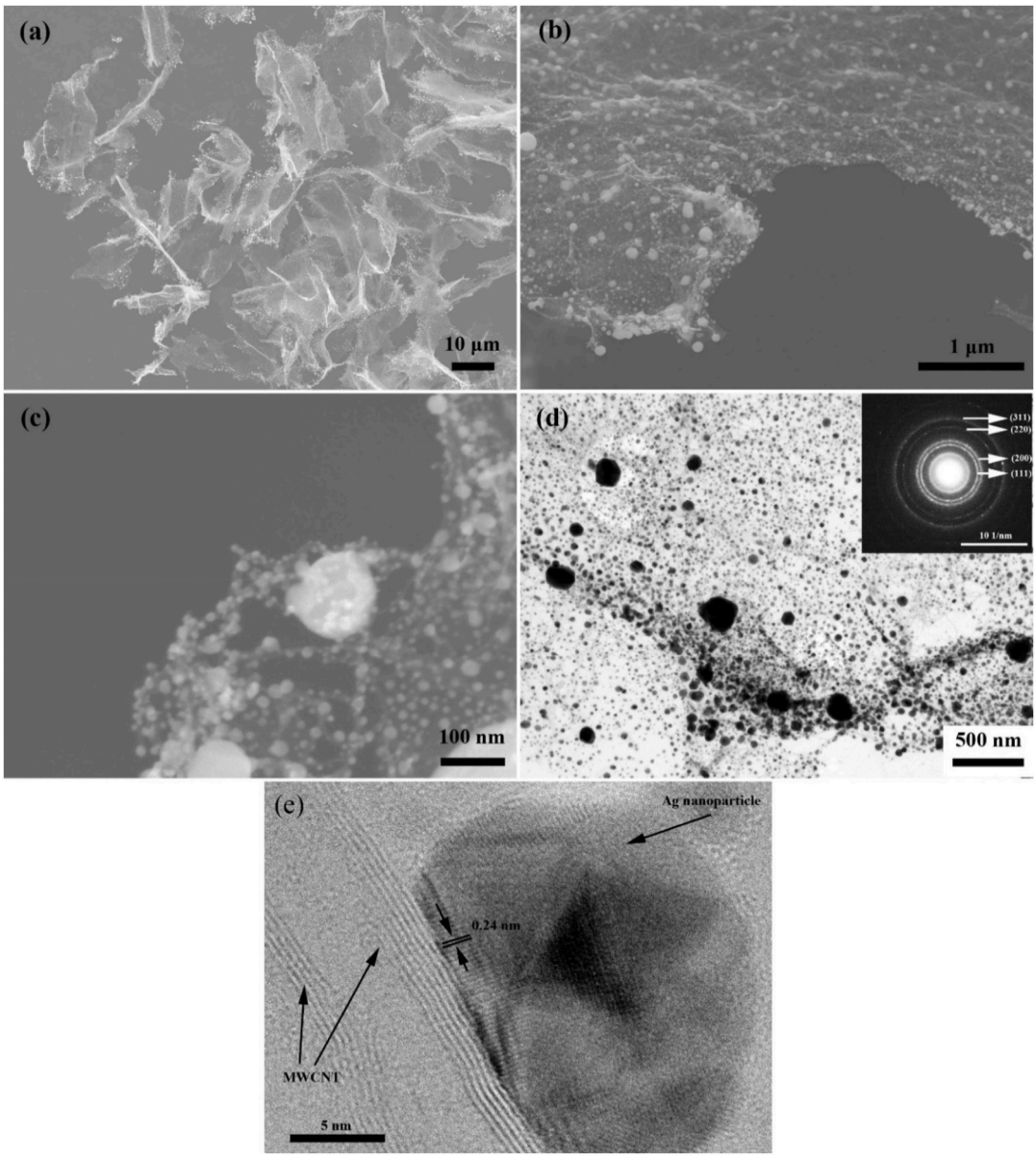

Fig. 3. SEM images of AgGNT nanostructures (a, b and c), and TEM images (d and e) of AgGNT nanostructures, the insert image of Fig. 2d is the electron diffraction (SAED) patterns.

and b. A similar squamous like morphology can be observed in both images, and no obvious contrast could be detected as they are both carbonaceous materials. Compared with the GNT-PEEK composites, the BSE image of Ag-PEEK composites (Fig. S3d) shows a more pronounced contrast of Ag particles in the PEEK matrix. The Ag particles have a poor dispersity compared with AgGNT-PEEK composites (Fig. 5d), as the Ag particles show apparent agglomeration both in Fig. S2 a and b and the subsequent dispersion process cannot disperse Ag particles effectively among PEEK matrix. Thus, it can be regarded that the AgGNT nanostructures are successfully added as fillers in the PEEK matrix with good dispersion among the matrix. The well-dispersed GNT structure makes the Ag nanoparticles uniformly distributed and formed a 3D network in the PEEK matrix, especially compared with the pure Ag sample (Fig. S3 a and b).

To further investigate the morphology of the AgGNT nanostructures in the PEEK matrix, the TEM images are displayed in Fig. 6. In Fig. 6a, the AgGNT nanostructures can be observed embedded in the PEEK matrix, and the AgGNT nanostructures still keep the graphene-layer-like structure. The morphology of AgGNT nanostructure embedded in PEEK matrix shows no obvious change compared with as-prepared AgGNT sample (Fig. 3), indicating that the whole disc preparation process did not destroy the AgGNT structure. Meanwhile, Table S1 displays the measured densities of all four samples through the Archimedes' principle, and the density of AgGNT-PEEK sample is 1.74 g cm^{-3} (equals around 99.4% of theoretic density). In the high-resolution image (Fig. 6b), the heads of carbon nanotubes and Ag particles can be clearly observed, and no apparent voids can be found between the PEEK and the AgGNT nanostructures. Thus, there is a good interface between the AgGNT nanostructures and the PEEK matrix. To further investigate the interface between nanostructures and PEEK matrix, XPS C1s spectra and their deconvolution peaks of pure PEEK, Ag-PEEK and AgGNT-PEEK samples have been obtained. In Fig. S4, the *C*–C peak for all three samples can be clearly found at the binding energy of around 284.6 eV. Both pure PEEK and Ag-PEEK samples show similar deconvolution peaks, the *C*–O peak at around 286.2 eV and the sp^2 hybrid orbit of benzene plane (π-π^*) in PEEK at around 292.0 eV [24,25]. There is no obvious difference between PEEK and Ag-PEEK samples, indicating that no evidence of interface between Ag and PEEK has been detected. In

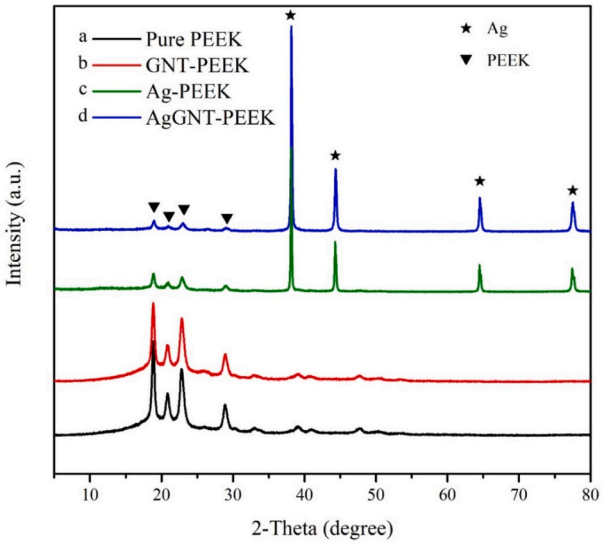

Fig. 4. The XRD patterns of pure PEEK (a), GNT-PEEK (b), Ag-PEEK (c), and AgGNT-PEEK (d).

Fig. S4c, an obvious intensity increase of the broad peak at around 292.0 eV can be observed. Although AgGNT nanostructures also showed sp^2 hybrid orbit of benzene plane at 291.5 eV, the significantly increased intensity for the broad peak at around 292.0 eV can be ascribed to the interface reaction between AgGNT and PEEK. It is likely that when the carbon hexagonal-ring of AgGNT nanostructures faced the benzene planes of PEEK, a chemical bond via π-π stacking formed and hence resulted in the much stronger peak [26].

3.2. Thermogravimetric and DSC analysis of PEEK-based composites

Thermogravimetric analysis (TGA) was used to investigate the thermal stability of all the PEEK-based composites in the inert (Ar) atmosphere, and the results are shown in Fig. 7a. A rapid decomposition stage at around 590 °C can be observed in all four samples, and the weights for all samples also become stable after 800 °C. The residual weight percentage of pure PEEK sample is around 52.4%, which can be regarded as the remaining ether and aromatic structures [4]. The remaining weight percentage of the GNT-PEEK sample is 55.6%, and it is 63.7% for the Ag-PEEK sample and 68.7% for the AgGNT-PEEK sample, respectively. The increase of remaining weight in these three composite samples can be ascribed to the adding of different weight percentage of fillers which cannot decompose under inert atmosphere. Differential scanning calorimetry (DSC) was adopted to explore the melting process, and the results are shown in Fig. 7b and Table 1. In Fig. 7b, a prominent endothermic peak from DSC measurements can be detected in all samples, indicating the melting temperature of PEEK during ramping [26]. The heat of fusion (ΔH_f) during melting for pure PEEK is 41.18 J g^{-1}, and this figure decrease to 38.44 J g^{-1} for GNT-PEEK composite, 32.48 J g^{-1} for Ag-PEEK composite and 29.28 J g^{-1} for AgGNT-PEEK composite. This decrease of ΔH_f can also be ascribed to the decline of PEEK amount in different composites. By comparing the ΔH_f of AgGNT-PEEK composite with the pure PEEK, the calculated weight ratio of AgGNT in the composites is around 28.9 wt % which is also consistent with the initial design in the sample preparation process.

3.3. Thermal and electrical conduction performances

The thermal diffusivity and conductivity of all four PEEK based samples are detailed in Fig. 8 a and b, while the relevant specific data are displayed in Table S1. In Fig. 8a, the thermal diffusivities increase after the addition of each filler. The AgGNT-PEEK composite shows the

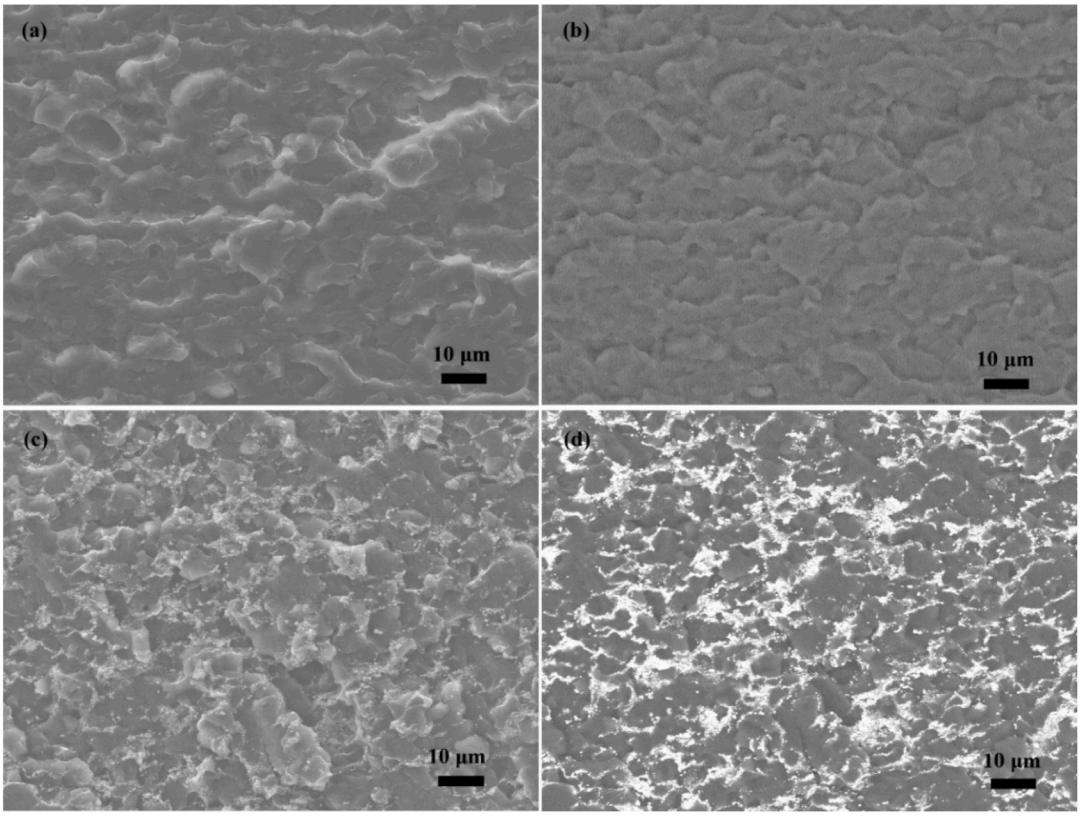

Fig. 5. The secondary electron SEM image of the pure PEEK (a) and AgGNT-PEEK (c) composites; The backscattering SEM image of the pure PEEK (b) and AgGNT-PEEK (d) composites.

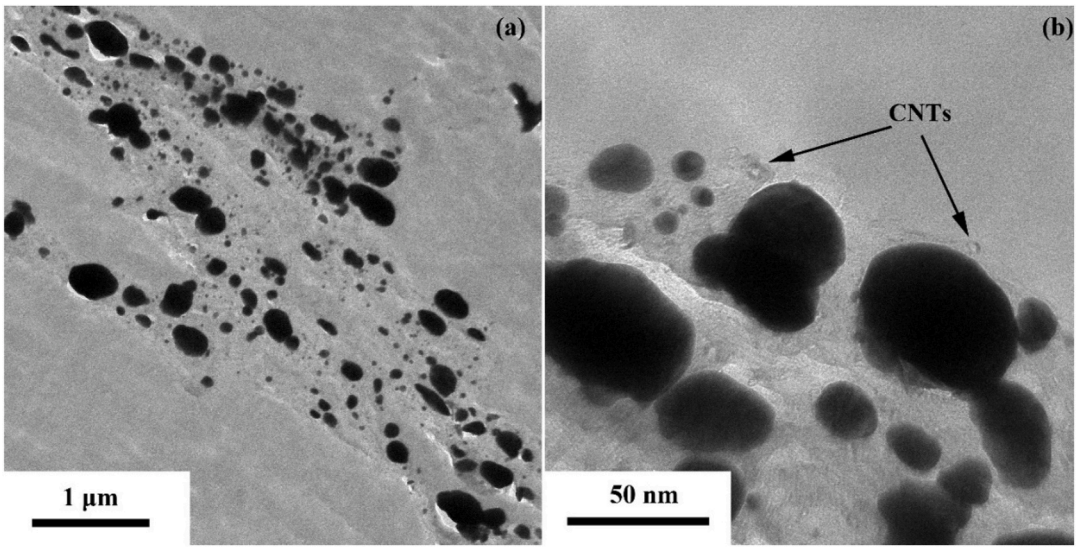

Fig. 6. TEM images (a and b) of AgGNT-PEEK composites.

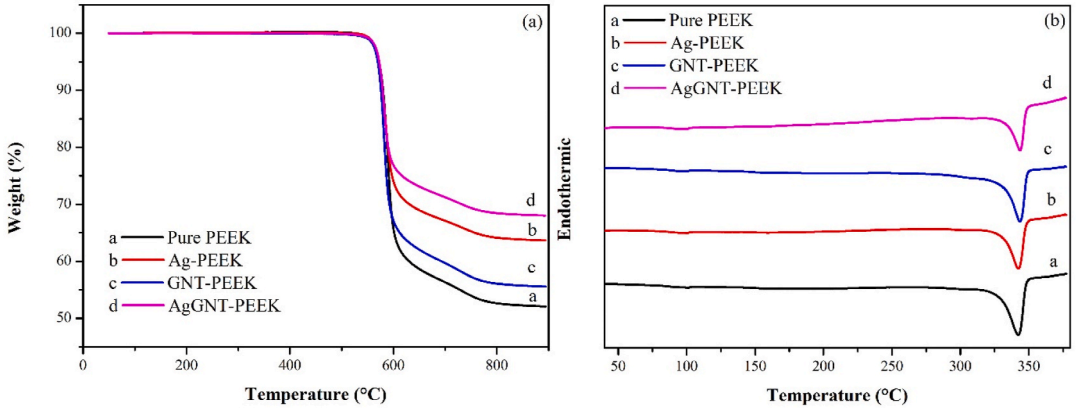

Fig. 7. TGA (a) and DSC curves of pure PEEK, GNT-PEEK, Ag-PEEK, and AgGNT-PEEK composites.

Table 1
The heat of fusion and melt temperature of pure PEEK, GNT-PEEK, Ag-PEEK, and AgGNT-PEEK composites.

Sample	ΔH_f (J g^{-1})	T_m (°C)
Pure PEEK	41.18	343.94
Ag-PEEK	32.48	343.21
GNT-PEEK	38.44	344.27
AgGNT-PEEK	29.28	344.47

highest value (0.255 mm^2 s^{-1}), while this value decreases to 0.194 mm^2 s^{-1} for Ag-PEEK and 0.195 mm^2 s^{-1} for GNT-PEEK, all higher than pure PEEK (0.180 mm^2 s^{-1}). The obtained thermal conductivities of all samples, which could be calculated by the equation $K = \alpha \times \rho \times C_p$, are shown in Fig. 8b. The pure PEEK sample exhibit a thermal conductivity of 0.270 W $m^{-1}K^{-1}$, which is similar to the reported values [15,26]. After the addition of pure Ag particles, the thermal conductivity increases to 0.354 W $m^{-1}K^{-1}$, as the Ag phase has a relatively high theoretic thermal conductivity than PEEK, while the GNT-PEEK composite illustrates the thermal conductivity of 0.310 W $m^{-1}K^{-1}$, which is lower than the Ag-PEEK composites. Meanwhile, the AgGNT-PEEK composite exhibits the best thermal conductivity (0.431 W $m^{-1}K^{-1}$, which is almost 60% higher than the pure PEEK) among the four samples, although it has the same weight amount of fillers when compared with Ag-PEEK and GNT-PEEK composites. Thus, combined with the SEM results (Fig. 5), it can be presumed that a well-dispersed 3D network structure of AgGNT-PEEK nanostructures was obtained among the PEEK matrix, and this 3D network provided continuous pathways for phonon and hence exhibited the best heat transfer. By combining the Ag and GNT, the perfect thermal conduction of Ag can be brought together with the 3D network that largely increased the thermal conductivity in AgGNT-PEEK composites (Fig. 8b).

The electrical conduction performances of these composites are investigated through ModuLab XM Materials Test System and the results are shown in Fig. 9. The electrical resistivities of all four composites decreased after the addition of fillers (Fig. 9), especially the GNT and AgGNT reinforced samples (from 5.8×10^{10} Ω m of pure PEEK to 1.8×10^2 and 11 Ω m, respectively). For the pure PEEK sample, the high electrical resistivity (5.8×10^{10} Ω m) indicates that the pure PEEK sample is an insulator. After the addition of 3.82 vol% (24 wt%) of Ag particles, there is a slight decrease of electrical resistivity to 3×10^{10} Ω m. Such minor decrease can be ascribed to the random distribution of Ag particles, which can be regarded as isolated islands in the PEEK matrix. According to previous research [15], it was shown that the electrical resistivity of PEEK/Ag composite would be significantly improved over 10.8 vol% of Ag nanoparticles (a sudden increase from around 10^{15} to 10 Ω m). This huge enhancement can be ascribed to the electrical percolation threshold. Thus, the Ag particle enhanced PEEK composites cannot exhibit a good electrical conduction performance unless a good connection was achieved between each Ag particles in the PEEK matrix.

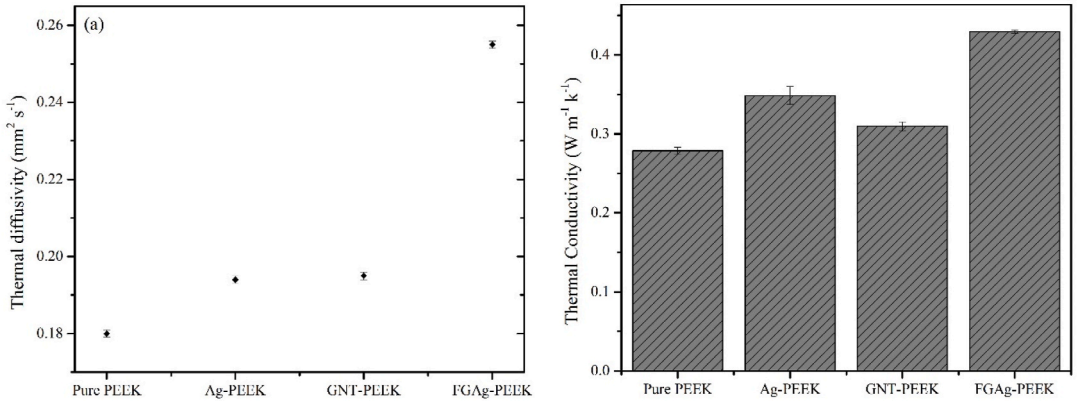

Fig. 8. The thermal diffusivity (a) and thermal conductivity (b) of pure PEEK, Ag-PEEK, GNT-PEEK and AgGNT-PEEK samples.

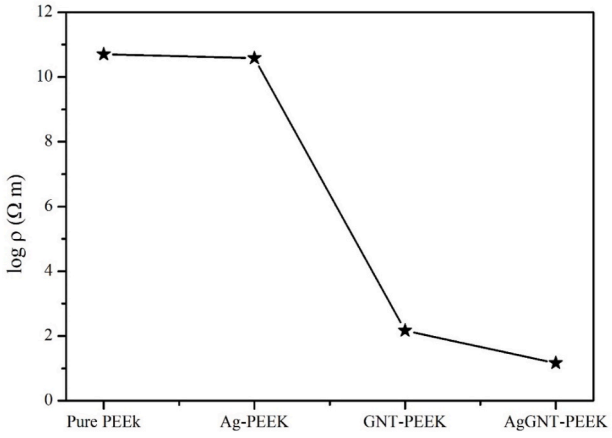

Fig. 9. The electrical resistivity of pure PEEK, Ag-PEEK, GNT-PEEK, and AgGNT-PEEK samples.

In the GNT-PEEK composites, there is a sharp decrease of electrical resistivity in which the value reaches 1.8×10^2 Ω m with only 4.04 vol% (6 wt%) of GNTs fillers, while the electrical resistivity is ca. 10^{13} Ω m for 4 vol% PEEK-AgNP composites in reference [15]. This huge improvement can be ascribed to the GNT nanostructure, which works as a 3D network and provides pathways for electron transfer. The previous research also showed that a percolation threshold always occurred between 3 wt% - 4 wt% in the carbon material (i.e., CNTs) [11], but the obtained best result was still 10^3 Ω m, which is still lower than the GNT-PEEK composites in our research (1.8×10^2 Ω m). A similar phenomenon has been reported in the graphene-PEEK system, the graphene-PEEK showed a significant electrical conduction enhancement from around 10^{12} Ω m (2 wt%) to 10^3 Ω m (3 wt%) and the authors also ascribed this improvement to a conductive network formed by graphene [27]. After the addition of AgGNT nanostructures, the AgGNT-PEEK sample displays an extra enhancement even compared with GNT-PEEK composites, which drops to around 10 Ω m. This further improvement can be ascribed to the introduction of Ag nanoparticles, which were uniformly coated on the GNT structure.

Table 2 presents the comparison of thermal and electrical performances between the AgGNT-PEEK composites and some reported results. Although few reports focused on both the thermal and electrical conduction performances with PEEK based composites, it still can be found that the AgGNT-PEEK composites displayed superior thermal and electrical conduction performances compared with either CNT or graphene reinforced PEEK composites [2,11,16,27–32]. Meanwhile, the Ag NP-PEEK composites showed poor performances (ca. 0.30 W m^{-1}K^{-1}) because of the isolated distribution of Ag nanoparticles [16], which is similar to the Ag-PEEK composites in this research. The authors also found that the Ag NWs formed a random dispersion in the 3 dimensions which resulted in a better electrical and thermal transport performance compared to Ag NPs [15,16]. It is interesting to notice that the enhancements of samples' electrical conductivities, no matter in this study or in other reports, are much higher than the enhancements of thermal conductivities [9,16]. This is due to different conduction theories, heat is always carried by acoustic phonons in polymer, while electricity is always transferred by electrons. Once a conductive pathway is formed in the polymer matrix, no matter it is made up by metal or nano-carbon networks, it will be more beneficial for the conduction of electrons [9,16]. Owing to the 3D network formed by the GNT nanostructure and the uniform decoration of Ag nanoparticles, the AgGNT nanostructures could largely enhance the thermal and electrical conduction performances of the PEEK matrix though the AgGNT-PEEK and Ag-PEEK composites have the same weight percentage of Ag.

Table 2
Comparison of thermal and electrical conduction performances between results in this work and previous results.

Sample	Thermal conductivity (W m^{-1}K^{-1})	Electrical resistivity (Ω m)	Reference
AgGNT-PEEK	0.43	10	This work
Ag-PEEK	0.35	3×10^{10}	This work
GO in PEEK	0.35	–	[2]
CNT-PEEK	–	10^4	[11]
MWCNT-PEEK	–	6×10^2	[28]
CNT-PEEK	–	9×10^3	[29]
PEEK/graphene/carbon fibre	0.38	–	[32]
Graphene-PEEK	–	10^4	[27]
Carbon fibre-PEEK	0.21	10^6	[30]
Graphene/carbon loofah/PEEK	–	10^2	[31]
Ag NPs-PEEK	0.30	10^{13}	[16]

3.4. Thermal durability analysis

As an important index of short-term heat resistance of PEEK, the thermal durability performances of the obtained PEEK-based composites and the effect of AgGNT nanostructures in the matrix were carried out by TMA analysis, and the results are displayed in Fig. 10. Under the pressure of 10^3 Pa (Fig. 10a), an initial increase of dimension can be observed after 300 °C in all samples, which can be ascribed to the sample expansion [3]. Meanwhile, the pure PEEK and Ag-PEEK samples displayed a sharp dimension change after 340 °C, which is the melting temperature (as shown in Table 1). The dramatic decrease of measured thickness indicated that the obtained disc melted and spread under 10^3 Pa, and finally the disc structure collapsed. However, both the

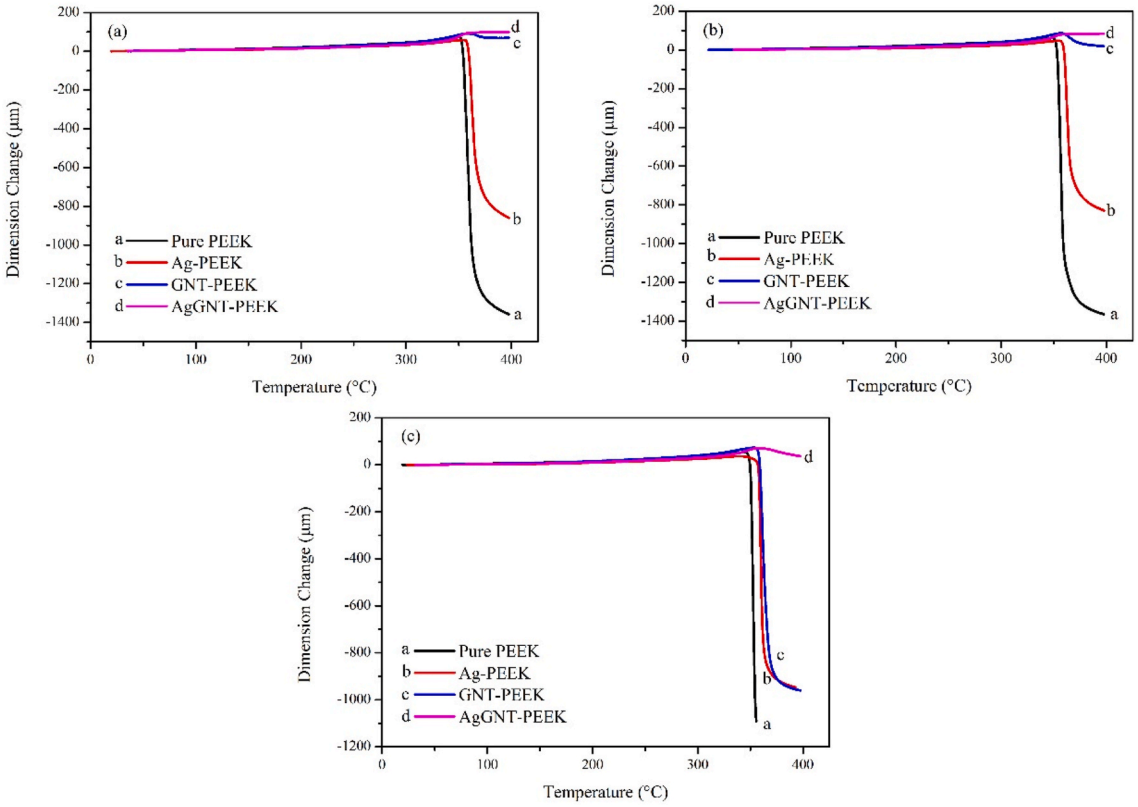

Fig. 10. The dimension change vs temperature of pure PEEK, Ag-PEEK, GNT-PEEK, and AgGNT-PEEK discs under different pressure: (a) 10^3 Pa, (b) 5×10^3 Pa and (c) 10^4 Pa.

GNT-PEEK and AgGNT-PEEK discs did not show noticeable changes up to 400 °C, which is above the melting temperature under 10^3 Pa, indicating that the initial structures of the GNT-PEEK and AgGNT-PEEK discs remained under the pressure of 10^3 Pa. When the pressure increases to 5×10^3 Pa (Fig. 10b), a similar result can be observed in all four samples, the pure PEEK and Ag-PEEK composite melted after 340 °C and the dimension of both discs decreased dramatically, while the GNT-PEEK and AgGNT-PEEK samples still did not show large dimension change. However, when the pressure increased to 10^4 Pa (Fig. 10c), the dimension of GNT-PEEK composite dramatically decreased, indicating

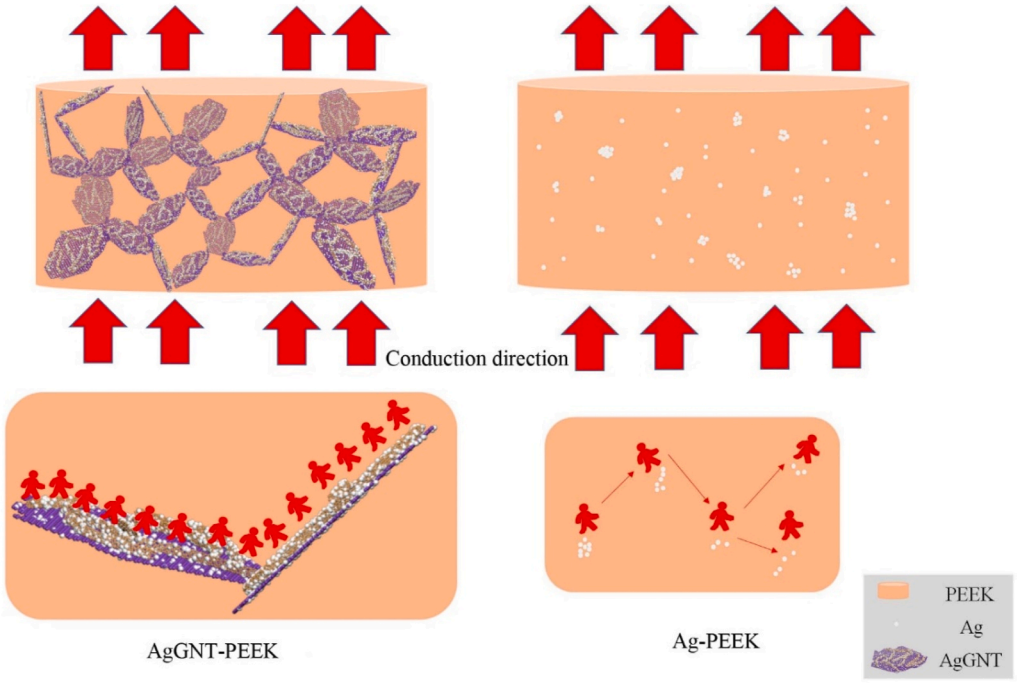

Fig. 11. Schematic of the 3D structure of AgGNT nanostructures in AgGNT-PEEK and the isolated Ag distribution in Ag-PEEK, and their conduction performances.

that the GNT-PEEK disc also collapsed under higher pressure. Meanwhile, there is still no obvious dimension change in the AgGNT-PEEK disc. Thus, the results indicate that the AgGNT nanostructures significantly improved the deflection temperature of the PEEK matrix under loads. Fig. S4 illustrates the picture of all four disc after 400 °C annealing for 2 h. It can be found that the pure PEEK and Ag-PEEK samples showed melt and the structure of the discs spread away. However, the GNT-PEEK sample kept the round disc structure and only a bubble can be observed on the surface, while the AgGNT-PEEK composite showed no visible change and kept the entire disc morphology. By considering the DSC results (Fig. 7b and Table 1), although all four composites showed obvious endothermic peaks at around 344 °C, the AgGNT nanostructures would reduce the fluidity of PEEK above melting temperature by forming 3D network in the matrix and hence improve the thermal durability.

The obtained results showed that the AgGNT-PEEK composite displayed excellent electrical and thermal conductivity as well as superior thermal durability even above the melting temperature of pure PEEK, especially compared with the pure PEEK, Ag or GNT-PEEK composites. As shown in Fig. 11, the 3D structures of AgGNT nanostructures have been generated in the PEEK matrix (Fig. 5), they acted as bridges that not only connected the Ag nanoparticles but also provided paths and channels that are beneficial to the electrical and thermal conduction performances. Meanwhile, the obtained pure Ag particles, which were prepared through the same process, were randomly distributed among the PEEK matrix (Fig. S3d and Fig. 11). Thus, the thermal and electrical conductivities of Ag-PEEK composites were lower than AgGNT-PEEK composites as the Ag particles could be regarded as isolated islands in the PEEK matrix. In addition, the AgGNT 3D network can be regarded as a skeleton in the PEEK matrix, which improved the deflection temperature and prevented the PEEK matrix structure from collapsing up to 400 °C under load, while the disc structures of pure PEEK, Ag-PEEK and GNT-PEEK composites were all pressed and collapsed. This is also an important index of the short-term heat resistance of PEEK. Thus, the AgGNT-PEEK composite displayed enhanced thermal and electrical conductivity and improved thermal durability and would make the PEEK-based sample much more reliable to be a potential option at high-temperature continuous-use for further application.

4. Conclusion

To conclude, uniform Ag nanoparticle decorated GNT nanostructures (AgGNT) were prepared through the MLM process with the subsequent freeze-drying and reduction methods. The obtained graphene-layer-like structure could prevent the agglomeration of Ag nanoparticles and keep a well-dispersed morphology during the subsequent composite preparation process. The AgGNT nanostructures were then utilised as the fillers in the PEEK matrix, and analysis of this AgGNT-PEEK nanostructure showed that a 3D network has been generated in the PEEK matrix. Because of this 3D network, the AgGNT-PEEK composites illustrated enhanced thermal conductivity (around 60% higher to pure PEEK) and significant improvement of electrical resistivity (form around 10^{-10} Ω m of pure PEEK to 10 Ω m of AgGNT-PEEK composites). Meanwhile, owing to this 3D AgGNT skeleton embedded among the PEEK matrix, the AgGNT-PEEK nanostructures also displayed enhanced thermal durability even above the melting temperature of pure PEEK. Thus, there is a great potential of utilising AgGNT nanostructures such as fillers to make PEEK widely applied in fields as semiconductors, high-temperature electrical application, aerospace and automobile industry.\

Author statement

Chenxi Hu: Conceptualization, Methodology, Formal analysis, Investigation, Writing - Original Draft.

Tianhui Liu: Investigation.

Nigel Neate: Investigation, Resources, Writing - Review & Editing.

Michael Fay: Investigation, Resources, Writing - Review & Editing.

Xianghui Hou: Resources, Supervision, Writing - Review & Editing.

David Grant: Supervision, Writing - Review & Editing.

Fang Xu: Conceptualization, Validation, Writing - Review & Editing, Supervision, Funding acquisition.

Declaration of competing interest

The authors declare that they have no known competing financial interests or personal relationships that could have appeared to influence the work reported in this paper.

Acknowledgments

This work is supported by a joint Ph.D. scholarship from the China Scholarship Council (CSC) and the University of Nottingham, and the Engineering and Physical Sciences Research Council [EP/L022494/1]. The authors also would like to acknowledge the technical assistance and instrumentation access from the Nanoscale and Microscale Research Centre (NMRC) at the University of Nottingham.

Appendix A. Supplementary data

Supplementary data to this article can be found online at https://doi.org/10.1016/j.compscitech.2021.109201.

References

[1] A.M. Díez-Pascual, M. Naffakh, M.A. Gómez, C. Marco, G. Ellis, M.T. Martínez, A. Ansón, J.M. González-Domínguez, Y. Martínez-Rubi, B. Simard, Development and characterization of PEEK/carbon nanotube composites, Carbon 47 (13) (2009) 3079–3090.

[2] Y. Hwang, M. Kim, J. Kim, Improvement of the mechanical properties and thermal conductivity of poly (ether-ether-ketone) with the addition of graphene oxide-carbon nanotube hybrid fillers, Compos. Appl. Sci. Manuf. 55 (2013) 195–202.

[3] S. Ata, Y. Hayashi, T.B.N. Thi, S. Tomonoh, S. Kawauchi, T. Yamada, K. Hata, Improving thermal durability and mechanical properties of poly (ether ether ketone) with single-walled carbon nanotubes, Polymer 176 (2019) 60–65.

[4] A.M. Díez-Pascual, M. Naffakh, J.M. González-Domínguez, A. Ansón, Y. Martínez-Rubi, M.T. Martínez, B. Simard, M.A. Gómez, High performance PEEK/carbon nanotube composites compatibilized with polysulfones-I. Structure and thermal properties, Carbon 48 (12) (2010) 3485–3499.

[5] J. Hay, D. Kemmish, Thermal decomposition of poly (aryl ether ketones), Polymer 28 (12) (1987) 2047–2051.

[6] R. Selzer, K. Friedrich, Mechanical properties and failure behaviour of carbon fibre-reinforced polymer composites under the influence of moisture, Compos. Appl. Sci. Manuf. 28 (6) (1997) 595–604.

[7] E.A. Hassan, D. Ge, L. Yang, J. Zhou, M. Liu, M. Yu, S. Zhu, Highly boosting the interlaminar shear strength of CF/PEEK composites via introduction of PEKK onto activated CF, Compos. Appl. Sci. Manuf. 112 (2018) 155–160.

[8] S.Y. Yang, K.H. Chang, H.W. Tien, Y.F. Lee, S.M. Li, Y.S. Wang, J.Y. Wang, C.C. M. Ma, C.C. Hu, Design and tailoring of a hierarchical graphene-carbon nanotube architecture for supercapacitors, J. Mater. Chem. 21 (7) (2011) 2374–2380.

[9] S. Stankovich, D.A. Dikin, G.H. Dommett, K.M. Kohlhaas, E.J. Zimney, E.A. Stach, R.D. Piner, S.T. Nguyen, R.S. Ruoff, Graphene-based composite materials, nature 442 (7100) (2006) 282.

[10] A.A. Balandin, S. Ghosh, W. Bao, I. Calizo, D. Teweldebrhan, F. Miao, C.N. Lau, Superior thermal conductivity of single-layer graphene, Nano Lett. 8 (3) (2008) 902–907.

[11] M. Mohiuddin, S. Hoa, Temperature dependent electrical conductivity of CNT–PEEK composites, Compos. Sci. Technol. 72 (1) (2011) 21–27.

[12] A. Tewatia, J. Hendrix, Z. Dong, M. Taghon, S. Tse, G. Chiu, W.E. Mayo, B. Kear, T. Nosker, J. Lynch, Characterization of melt-blended graphene–poly (ether ether ketone) nanocomposite, Mater. Sci. Eng., B 216 (2017) 41–49.

[13] J.L. Zeng, F.R. Zhu, S.B. Yu, L. Zhu, Z. Cao, L.X. Sun, G.R. Deng, W.P. Yan, L. Zhang, Effects of copper nanowires on the properties of an organic phase change material, Sol. Energy Mater. Sol. Cell. 105 (2012) 174–178.

[14] J. Zeng, Z. Cao, D. Yang, L. Sun, L. Zhang, Thermal conductivity enhancement of Ag nanowires on an organic phase change material, J. Therm. Anal. Calorim. 101 (1) (2010) 385–389.

[15] L. Rivière, A. Lonjon, E. Dantras, C. Lacabanne, P. Olivier, N.R. Gleizes, Silver fillers aspect ratio influence on electrical and thermal conductivity in PEEK/Ag nanocomposites, Eur. Polym. J. 85 (2016) 115–125.

[16] L. Rivière, N. Caussé, A. Lonjon, E. Dantras, C. Lacabanne, Specific heat capacity and thermal conductivity of PEEK/Ag nanoparticles composites determined by Modulated-Temperature Differential Scanning Calorimetry, Polym. Degrad. Stabil. 127 (2016) 98–104.

[17] Y. Zhang, Z. Wang, Y. Ji, S. Liu, T. Zhang, Synthesis of Ag nanoparticle–carbon nanotube–reduced graphene oxide hybrids for highly sensitive non-enzymatic hydrogen peroxide detection, RSC Adv. 5 (49) (2015) 39037–39041.
[18] F. Li, Y. Guo, Y. Liu, H. Qiu, X. Sun, W. Wang, Y. Liu, J. Gao, Fabrication of Pt–Cu/RGO hybrids and their electrochemical performance for the oxidation of methanol and formic acid in acid media, Carbon 64 (2013) 11–19.
[19] D. Li, M.B. Müller, S. Gilje, R.B. Kaner, G.G. Wallace, Processable aqueous dispersions of graphene nanosheets, Nat. Nanotechnol. 3 (2) (2008) 101.
[20] J. Yu, T. Ma, S. Liu, Enhanced photocatalytic activity of mesoporous TiO_2 aggregates by embedding carbon nanotubes as electron-transfer channel, Phys. Chem. Chem. Phys. 13 (8) (2011) 3491–3501.
[21] J. Li, S. Tang, L. Lu, H.C. Zeng, Preparation of nanocomposites of metals, metal oxides, and carbon nanotubes via self-assembly, J. Am. Chem. Soc. 129 (30) (2007) 9401–9409.
[22] C. Zhang, L. Ren, X. Wang, T. Liu, Graphene oxide-assisted dispersion of pristine multiwalled carbon nanotubes in aqueous media, J. Phys. Chem. C 114 (26) (2010) 11435–11440.
[23] J. Puértolas, M. Castro, J. Morris, R. Ríos, A. Ansón-Casaos, Tribological and mechanical properties of graphene nanoplatelet/PEEK composites, Carbon 141 (2019) 107–122.
[24] P. Louette, F. Bodino, J.-J. Pireaux, Poly (ether ether ketone)(PEEK) XPS reference core level and energy loss spectra, Surf. Sci. Spectra 12 (1) (2005) 149–153.
[25] Y. Hong, J.W. Lam, B.Z. Tang, Aggregation-induced emission, Chem. Soc. Rev. 40 (11) (2011) 5361–5388.
[26] N. Wang, Z. Yang, K. Thummavichai, F. Xu, C. Hu, H. Chen, Y. Xia, Y. Zhu, Novel graphitic carbon coated IF-WS_2 reinforced poly (ether ether ketone) nanocomposites, RSC Adv. 7 (56) (2017) 35265–35273.
[27] A. Martínez-Gómez, S. Quiles-Díaz, P. Enrique-Jimenez, A. Flores, F. Ania, M. A. Gómez-Fatou, H.J. Salavagione, Searching for effective compatibilizing agents for the preparation of poly (ether ether ketone)/graphene nanocomposites with enhanced properties, Compos. Appl. Sci. Manuf. 113 (2018) 180–188.
[28] Y.J. Lin, S. Qin, B. Han, C. Gao, S.L. Zhang, Preparation of poly (ether ether ketone)-based composite with high electrical conductivity, good mechanical properties and thermal stability, High Perform. Polym. 29 (2) (2017) 205–210.
[29] M. Mohiuddin, S.V. Hoa, Estimation of contact resistance and its effect on electrical conductivity of CNT/PEEK composites, Compos. Sci. Technol. 79 (2013) 42–48.
[30] A. Saleem, L. Frormann, A. Iqbal, High performance thermoplastic composites: study on the mechanical, thermal, and electrical resistivity properties of carbon fiber-reinforced polyetheretherketone and polyethersulphone, Polym. Compos. 28 (6) (2007) 785–796.
[31] S. Li, W. Li, J. Nie, D. Liu, G. Sui, Synergistic effect of graphene nanoplate and carbonized loofah fiber on the electromagnetic shielding effectiveness of PEEK-based composites, Carbon 143 (2019) 154–161.
[32] L. Liu, L. Xiao, X. Zhang, M. Li, Y. Chang, L. Shang, Y. Ao, Improvement of the thermal conductivity and friction performance of poly (ether ether ketone)/carbon fiber laminates by addition of graphene, RSC Adv. 5 (71) (2015) 57853–57859.